

JMRI, 2025; Vol. 46 No.3: (10-22)

Journal of the Medical Research Institute

Diosmin Mitigates Sodium Arsenite-Induced Reproductive Dysfunction via Oxidative/Inflammatory Modulation and AKT/ERK Pathways in Male Rats.

yasmine Khaled Mohamed 1, Nema Mohammed Abd El-Hameed 1, Hussein Khamis Hussein 1, Heba Mohamed Abdou 1*

1) Zoology Department, Faculity of Science, Alexandria University, Egypt.

ABSTRACT:

Arsenic (As), a ubiquitous environmental contaminant, poses a significant threat to human health. Diosmin (DIO), a natural flavone glycoside found in citrus fruits. This study inspected the protective effects of DIO against Asinduced testicular toxicity in adult male rats, with emphasis on oxidative stress, inflammation, and AKT/ERK signaling pathways. Twenty-four adult male albino rats were randomly assigned into four groups: control, As (10 mg/kg BW /day), As+DIO (10 mg/kg BW As + 200 mg/kg BW DIO/day), and DIO-only (200 mg/kg BW /day), orally for 35 days. As exposure significantly impaired sperm parameters, reduced reproductive hormone levels [gonadotropin-releasing hormone (GnRH), testosterone, follicle-stimulating hormone (FSH), and luteinizing hormone (LH)], and decreased steroidogenic enzymes. It also elevated oxidative stress [thiobarbituric acid reactive substances (TBARS)], inflammatory markers [nuclear factor kappa B (NF-κB) and tumor necrosis factor-alpha (TNF-α)], protein kinase B/extracellular signal-regulated kinase (AKT/ERK) signaling, and caspase-3 expression, while suppressing antioxidant enzymes [reduced glutathione (GSH), superoxide dismutase (SOD), and catalase (CAT)]. Co-treatment with diosmin (DIO) markedly restored antioxidant balance, reduced inflammation, normalized hormone and enzyme levels, and improved AKT/ERK signaling. Histological analysis confirmed structural recovery in testicular tissues and reduced caspase-3 expression.

These results highlight DIO's potential to counteract As-induced reproductive toxicity by modulating oxidative stress, inflammation, and key signaling pathways, supporting its therapeutic value in protecting male reproductive health.

Keywords: Diosmin; Arsenite; Oxidative Regulation; impaired steroidogenesis; apoptosis.

1. INTRODUCTION

Arsenic, a ubiquitous environmental contaminant, poses a significant threat to human health, with sodium arsenite (As) being a particularly potent form inducing severe toxicity across various organ systems (Ganie et al., 2024). Reproductive toxicity is a major concern, as As exposure has been

consistently linked to impaired spermatogenesis, hormonal imbalances, and compromised fertility in both humans and experimental animals (Renu et al., 2018). The primary mechanisms underlying As-induced reproductive dysfunction involve the generation of reactive oxygen species (ROS), leading

to oxidative stress, and the activation of inflammatory pathways (Choudhary et al., 2024). These processes disrupt the delicate balance of testicular function, affecting steroidogenesis, sperm maturation, and overall reproductive capacity.

Oxidative stress, characterized by an imbalance between ROS production and antioxidant defenses, plays a pivotal role in As-mediated testicular damage. As exposure depletes endogenous antioxidants such as glutathione (GSH), superoxide dismutase (SOD), catalase (CAT), while simultaneously increasing lipid peroxidation, indicated by elevated thiobarbituric acid reactive substances (TBARS) (Rachamalla et al., 2022). Furthermore, As triggers inflammatory responses through the activation of nuclear factor kappa B (NF-κB) and the release of proinflammatory cytokines such as tumor necrosis factor-alpha (TNF-α) (Mohtadi et al., 2023 & Choudhary et al., 2024). These inflammatory mediators contribute to cellular damage and further exacerbate oxidative stress.

In addition to oxidative stress and inflammation, As exposure disrupts critical cellular signaling pathways, including the Protein Kinase B (Akt) and Extracellular Signal-Regulated Kinase (ERK) pathways, which are essential for testicular function and germ cell survival (Yao et al., 2018; Mishra et al., 2024). Dysregulation of these pathways can lead to apoptosis of germ cells and impaired steroidogenesis, further contributing to reproductive toxicity.

Diosmin (DIO), a naturally occurring flavonoid found in citrus fruits, has garnered significant attention due to its potent antioxidant and anti-inflammatory properties (Malayeri et al., 2024; Ahmed et al., 2016). Previous studies have demonstrated that DIO can effectively scavenge ROS, enhance antioxidant enzyme activity, and suppress inflammatory responses (Mohtadi et al., 2023; Oyovwi et al., 2024). Moreover, flavonoids have been shown to modulate gene expression and cellular signaling pathways, suggesting that DIO may offer a protective role against As-induced reproductive toxicity (Martin & Touaibia, 2020; Wang et al., 2021). Therefore, this study aimed to inspect the protective effects of diosmin against As-induced reproductive toxicity in male rats, focusing on the concerted action of oxidative/inflammatory regulation and AKT/ERK signaling.

2. Materials and Methods

2.1. Experimental animals and procedures

Twenty four adult male albino rats (approximately 11-12 weeks old, weighing (190-200g) were obtained from experimental animal center, medical research institute, Alexandria University, Alexandria, Egypt. The animals were housed in standard polypropylene cages under controlled environmental conditions (temperature $22 \pm 2^{\circ}$ C, humidity 50 \pm 10%, 12-hour light/dark cycle) with free access to standard rodent chow and water. All experimental procedures were conducted in accordance with the guidelines of the Institutional Animal Ethics Committee of Alexandria University, Egypt, and approved under protocol number AU 04 22 08 27 1 01

After a one-week acclimatization period, the rats were randomly divided into four groups (n=6 per group):

Control Group: Received vehicle (distilled water) orally. **As-Treated Group:** Received sodium arsenite (As, Alpha

Chemika for chemical industries, Mumbai India. (Cat. No AL4065) India, at a dose of 10 mg/kg body weight (BW) (Morakinyo et al., 2010) per day orally, dissolved in distilled water.

As+ DIO-Treated Group: Received As (10 mg/kg BW/day) and DIO was supplied by Nutrition Greenlife Co., New York, NY, USA. at a dose of 200 mg/kg BW/day (Habib et al., 2022) orally, both dissolved in distilled water.

DIO-Supplemented Group: Received DIO (200 mg/kg BW/day) orally, dissolved in distilled water.

All treatments were administered orally via gavage for 35 consecutive days.

2.2. Sample Collection and tissue homogenate preparation Twenty-four hours after the last treatment, the rats were anesthetized with a combination of ketamine (Ketalar, Pfizer, USA; 90 mg/kg) and xylazine (Xyla-Ject, Adwia, Egypt; 10 mg/kg). Blood samples were collected via cardiac puncture and centrifuged at 3000 rpm for 15 minutes at 4 °C to separate serum. The testes were immediately excised, weighed, and processed for various analyses. One testis from each animal was fixed in 10% formalin for histological and immunohistochemical studies. The contralateral testis was snap-frozen and stored at -80 °C for biochemical and gene expression analyses.

For biochemical analyses, the collected testicular tissues were carefully minced, rinsed with ice-cold PBS (pH 7.4), and

homogenized (10% w/v) using a Dounce glass homogenizer. The resulting homogenates were centrifuged at 2,000 rpm for 10 minutes at 4 $^{\circ}$ C, and the supernatants were collected and stored at -20 $^{\circ}$ C until subsequent biochemical evaluations.

2. 3. Biochemical assays:

2.3.1. Oxidative stress and antioxidant assessment:

Testicular lipid peroxidation was estimated by measuring thiobarbituric acid reactive substances (TBARS) according to Draper & Hadley, (1990). Briefly, testis homogenates were incubated with thiobarbituric acid in an acidic medium and heated, allowing malondialdehyde (MDA) to form a chromogenic complex. The absorbance was measured at 532 nm, and TBARS levels were expressed as nmol MDA equivalents per mg protein.

Reduced glutathione (GSH) levels were quantified as a major non-enzymatic antioxidant following the method described by Beutler et al. (1963). Briefly, GSH reacts with 5,5'-dithiobis(2-nitrobenzoic acid) (DTNB) to form a yellow-colored product, and the absorbance was measured spectrophotometrically to determine GSH concentration (BioDiagnostic, Egypt; Cat. No: GR 2511). Enzymatic antioxidant activities of superoxide dismutase (SOD) and catalase (CAT) were measured using commercially available kits (BioDiagnostic Co., Giza, Egypt; SOD: Cat. No. SD2521, CAT: Cat. No. CA2517). SOD activity was determined according to the method of Nishikimi et al. (1972), which relies on the inhibition of nitroblue tetrazolium (NBT) reduction by the superoxide anion. CAT activity was assayed following the method of Aebi (1984), based on the decomposition rate of hydrogen peroxide at 240 nm.

2.3.2. Inflammatory markers in testicular tissue:

The levels of NF- κ B and TNF- α in testicular tissue homogenates were quantified using commercially available Enzyme-Linked Immunosorbent Assay (ELISA) kits (NF- κ B: Cat. No. MBS453975; TNF- α : Cat. No. MBS282960; MyBioSource, San Diego, CA, USA) according to the manufacturer's protocols. The absorbance was measured at 450 nm using a microplate reader. These methods were performed following previously published protocols for NF- κ B (Lawrence, 2009) and TNF- α quantification (Balkwill, 2009), which validate ELISA as a reliable approach for inflammatory biomarker determination.

2.3.3. Lipid profile assessment:

Serum concentrations of total cholesterol, triglycerides, high-density lipoprotein cholesterol (HDL-C), and low-density lipoprotein cholesterol (LDL-C) were determined using commercially available colorimetric kits (Bio Diagnostic Co., Giza, Egypt; Cat. No. CH1220, TR2030, CH1230, and CH1231, respectively) following the manufacturer's instructions. The methodologies used for total cholesterol, triglycerides, HDL-C, and LDL-C estimation were based on previously published methods by Allain et al. (1974), Fossati & Prencipe (1982), Lopes-Virella et al. (1977), and Friedewald et al. (1972), respectively.

2.3.4. Hormonal and steroidal enzyme levels:

Serum concentrations of gonadotropin-releasing hormone (GnRH), testosterone, follicle-stimulating hormone (FSH), and luteinizing hormone (LH) were quantified using enzymelinked immunosorbent assay (ELISA) kits (MyBioSource,

USA; Cusabio, USA; FineTest, Wuhan, China; and Elabscience, USA; GnRH: Cat. Nos. MBS2020839 & CSB-E05100r, FSH: Cat. No. ER0960, LH: Cat. No. E-EL-R0026, respectively). These assays employ a quantitative sandwich ELISA format, in which target hormones are captured by specific antibodies, and the resulting colorimetric signal intensity is directly proportional to their concentrations (Han et al., 2022; Mahmoud et al., 2025; Hwang et al., 2025; Olojede et al., 2022, respectively). The enzymatic activities of 17β-hydroxysteroid dehydrogenase (17β-HSD) and 3βhydroxysteroid dehydrogenase (3β-HSD) in testicular tissues were also evaluated using sandwich ELISA kits (17β-HSD: Cat. No. MBS2707678, MyBioSource, USA; 3β-HSD: Cat. No. CSB-EL010781RA, Cusabio, USA) according to the manufacturers' instructions (Anwar et al., 2022; Kozłowska et al., 2019, respectively).

2.4. Sperm analysis:

Sperm collection was performed from the left cauda epididymis of each rat. The tissue was carefully dissected free of adhering connective tissue. To extract spermatozoa, the epididymis was minced in 5 mL of Ham's F12 medium and incubated for 5 min at 35 °C to allow for sperm dispersal. The resulting suspension was subjected to repeated washings in fresh Ham's F12 medium to isolate sperm for subsequent analysis. Sperm quality evaluation: encompassed three key parameters: count, motility, and morphology. Sperm concentration (×10⁶/mL) was determined using an improved Neubauer hemocytometer (Slott et al., 1991). A 10 μL aliquot of the washed suspension was loaded onto the chamber and allowed to settle for 10 min before counting. Percent motility

was assessed by examining at least ten separate fields on the hemocytometer under a phase-contrast microscope and calculating the ratio of progressively motile sperm to the total number of sperm (Essawy et al., 2024). Sperm morphology was assessed on air-dried smears stained with eosin-nigrosin. For each animal, one hundred spermatozoa were systematically examined at high magnification (×400) under a bright-field microscope, and the percentage of cells exhibiting abnormal head or flagellar morphology was recorded.

2.5. Quantitative Real-Time PCR

Gene expression levels of AKT (Thymoma viral oncogene) and ERK (Extracellular signal-Regulated Kinase) were quantified by one-step quantitative real-time PCR (qRT-PCR) using the QuantiTect SYBR Green RT-PCR Kit (Qiagen, Montgomery, MD, USA; cat. no. 204243). Total RNA was extracted from testicular tissues using TRIzol Reagent (Thermo Fisher Scientific, Waltham, MA, USA; cat. no. 15596-018) according to the manufacturer's instructions. Each 25 µL reaction mixture contained 2× SYBR Green RT-PCR Master Mix, QuantiTect RT Mix, template RNA (100 ng), gene-specific primers (Table 1), and RNase-free water. Thermal cycling was carried out on a Rotor-Gene real-time PCR system with the following program: reverse transcription at 55 °C for 10 min, initial denaturation at 95 °C for 5 min, followed by PCR amplification under optimized annealing/extension conditions for each primer set. Relative expression levels were calculated using the $2^{-\Delta\Delta Ct}$ method, with β-Actin as the reference gene (Livak & Schmittgen, 2001).

Table 1: The sequence of the Primer

Gene	Forward primer	Reverse primer
AKT	AGTCCCCACTCAACAACTTCT	GAAGGTGCGCTCAATGACTG
ERK	GAAGACACAGCACCTCAGCAA	TGGAAGGCTTGAGGTCACGGT
β-Actin	ATGTGGCTGAGGACTTTGATT	ATCTATGCCGTGGATACTTGG

According to Oguzoglu et al. (2024), Ramalingam et al. (2016), and Hassan *et al.* (2023) respectively. Accession number: XM 006240631.3, NM 053842.2, and XM 039089807.1, respectively

2.6. Histological and immunohistochemical analysis:2. 6.1. Histological Processing

Testes were collected, fixed in 10% neutral buffered formalin, and processed through standard dehydration, clearing, and paraffin embedding. Sections (5 μ m) were stained with hematoxylin and eosin (H&E) using established protocols. Histopathological examination was performed using light microscopy (Olympus CX41) with digital image capture (Olympus UTU1X-2).

2. 6.2. Immunohistochemical detection of apoptosis

Apoptotic activity in testicular tissues was assessed via caspase-3 immunohistochemistry using the avidin-biotin complex (ABC) method (Hsu et al., 1981). Following deparaffinization and rehydration, sections were treated with 0.3% hydrogen peroxide to quench endogenous peroxidase activity and blocked with 3% horse serum. Sections were incubated with a rabbit polyclonal anti-caspase-3 primary antibody (Abcam, ab4051; 1:20,000 dilution), followed by a

biotinylated secondary antibody and ABC reagent. Antigen localization was visualized using 3,3'-diaminobenzidine (DAB), yielding a brown precipitate. Sections were counterstained with hematoxylin, dehydrated, cleared, and mounted. Caspase-3 positivity—indicative of apoptosis—was identified as brown cytoplasmic staining under light microscopy.

2.7. Statistical analysis:

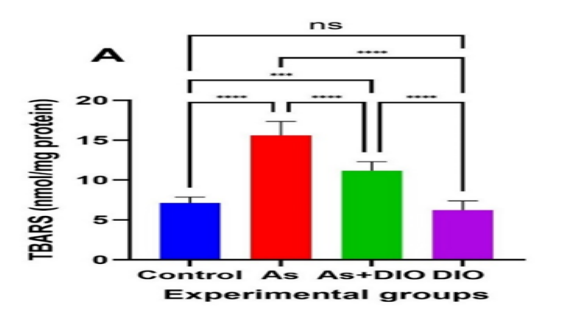
All data were statistically analyzed using IBM SPSS Statistics (Version 27.0, IBM Corp., Chicago, USA) and GraphPad Prism (Version 10.1.2, GraphPad Software Inc., San Diego, CA, USA). Group comparisons were conducted using one-way analysis of variance (ANOVA) followed by Tukey's post hoc test for multiple comparisons. Data are presented as mean \pm standard deviation (SD). Statistical significance was set at $p \le 0.05$, with higher levels of significance indicated at $p \le 0.01$, $p \le 0.001$, and $p \le 0.0001$.

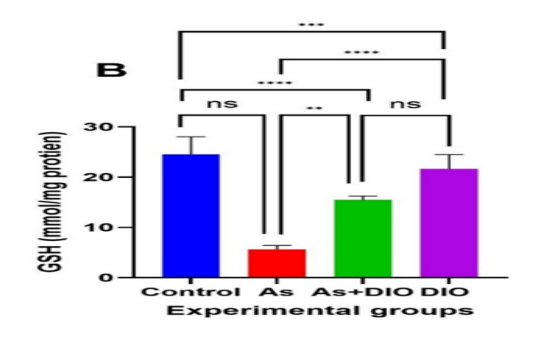
3. Results

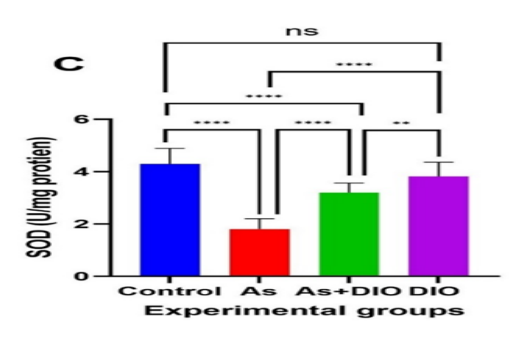
3.1. Effects on Oxidative Stress Markers and Antioxidant Enzymes

Exposure to sodium arsenite (As) triggered pronounced oxidative stress in testicular tissue. Rats subjected to As exhibited a significant increase (P < 0.05) in TBARS, indicating enhanced lipid peroxidation relative to controls (Figure 1A). This oxidative insult was accompanied by a marked reduction (P < 0.05) in key endogenous antioxidants, including GSH, SOD, and CAT (Figure 1B–D), reflecting a compromised antioxidant defense system.

Importantly, co-administration of diosmin (As + DIO) effectively mitigated these oxidative perturbations. TBARS levels were notably lowered, while GSH, SOD, and CAT activities were restored compared to the As-only group, demonstrating DIO's protective antioxidant potential. Rats receiving DIO alone displayed no significant changes in oxidative stress markers relative to controls, confirming that DIO does not disrupt redox homeostasis under normal conditions (Figure 1A–D).







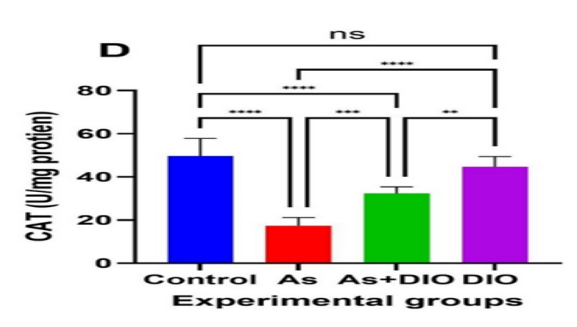
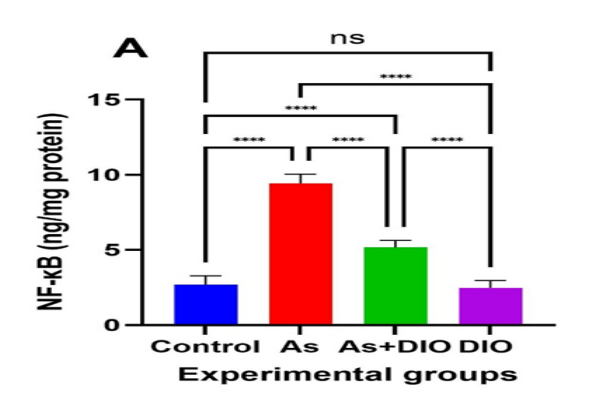


Figure (1) Evaluation of oxidative stress biomarkers, GSH, and the activities of antioxidant enzymes in the testis of different experimental groups. (A) TBARS, (B) GSH, (C) SOD and (D) CAT levels in testicular tissues. The results are exhibited as mean \pm SD when n=6, which were analyzed following one-way ANOVA associated with multiple comparisons between different groups adopting Tukey's test (**** p < 0.0001, *** p < 0.001, ** p < 0.01, and * p < 0.05). Abbreviations: GSH: glutathione; TBARS: thiobarbic acid reactive substance; SOD: superoxide dismutase; and CAT: catalase

3.2. Effects on Inflammatory Markers

As exposure notably increased (P < 0.05) the testicular levels of NF- κ B and TNF- α compared to controls (Figure 2A, B). This effect was markedly attenuated by DIO co-

administration, with the As + DIO group showing significantly lower concentrations than the As-only group. In the DIO-alone group, levels of these markers remained comparable to controls (Figure 2A, B).



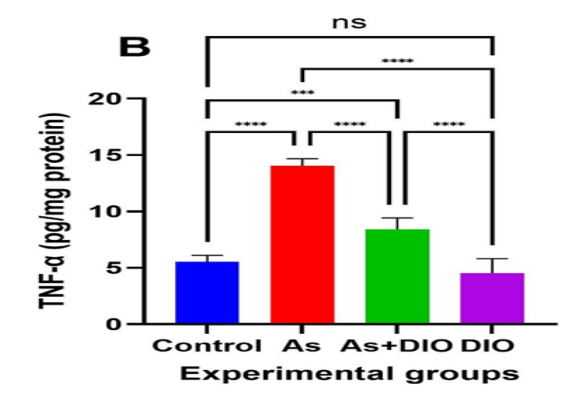


Figure (2) Estimation of inflammatory biomarkers in testis of different experimental groups. (**A**) NFkB (**B**) TNF- α in testicular tissues. The results are exhibited as mean \pm SD when n =6, which were analyzed following one-way ANOVA associated with multiple comparisons between different groups adopting Tukey's test (**** p < 0.0001, **** p < 0.001, *** p < 0.01, and * p < 0.05). Abbreviations: NFkB: nuclear factor kappa B; TNF- α : Tumor Necrosis Factor alpha

3.3. Effects on Sperm Quality, Reproductive Hormones, and Steroidogenic Enzymes

Treatment with As led to a significant (P < 0.05) decline in sperm count and motility, alongside a marked increase in the percentage of sperm with abnormal morphology (Figure 3A–C). Furthermore, a notable (P < 0.05) reduction was observed in serum levels of GnRH, testosterone, FSH, and LH, as well

as in the activities of the steroidogenic enzymes 17β -HSD and 3β -HSD (Figure 3D–I). Co-treatment with DIO markedly attenuated these As-induced deficits, bringing all parameters closer to normal levels. Treatment with DIO alone resulted in values that were statistically indistinguishable from those of the control group.

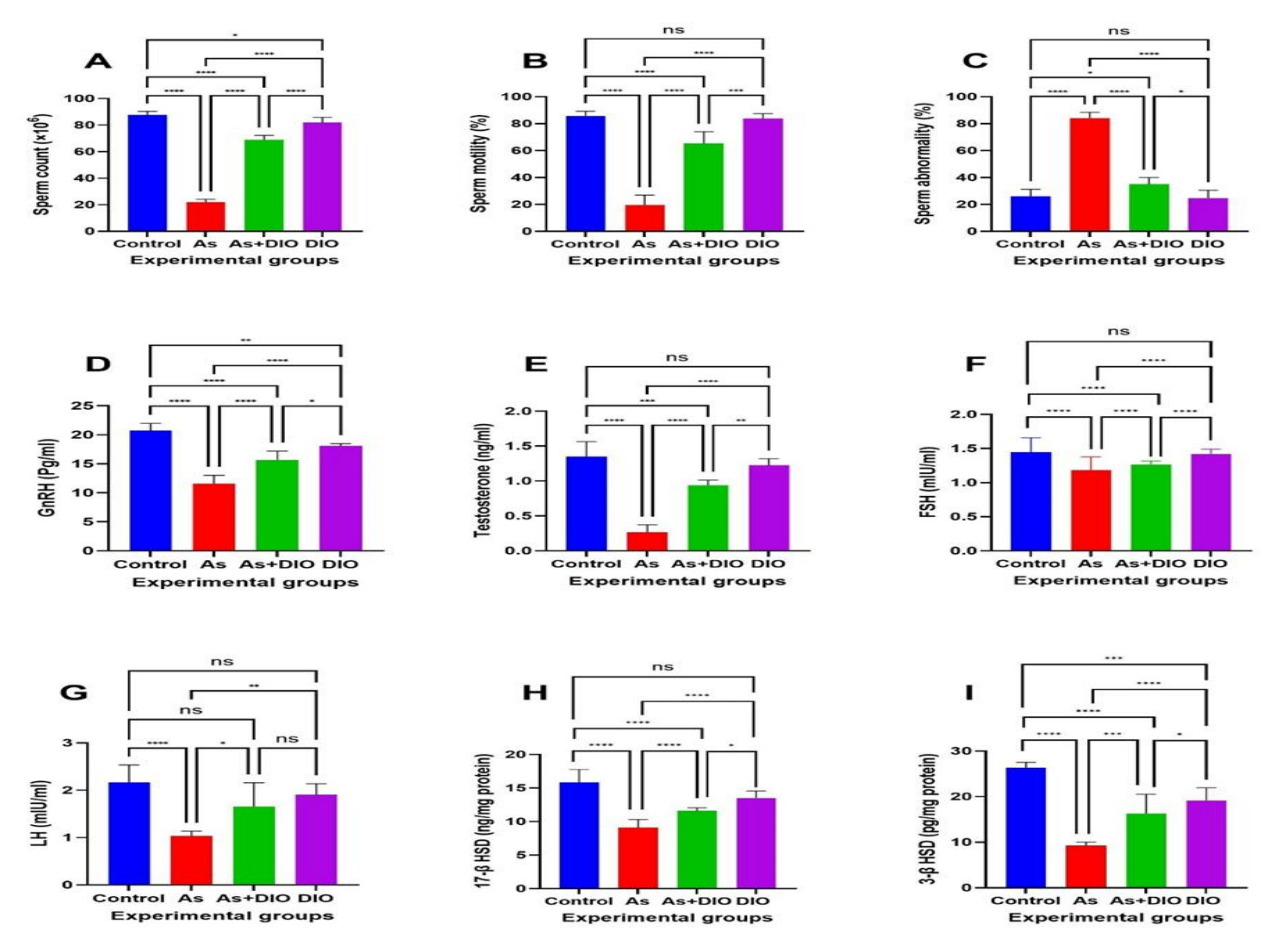


Figure (3) Determination of (A) sperm count, (B) sperm motility, (C) sperm abnormality, (D) GnRH, (E) Testosterone, (F) FSH, (G) LH, (H) 17- β HSD and (I) 3- β HSD in testis of different animal groups. The results are exhibited as mean ± SD when n =6, which were analyzed following one-way ANOVA associated with multiple comparisons between different groups adopting Tukey's test (**** p < 0.0001, *** p < 0.001, ** p < 0.01, and * p < 0.05). Abbreviations: GnRH: gonadotropin releasing hormone; FSH: follicle stimulating hormone; LH: luteinizing hormone; 17- β HSD: 17 β -Hydroxysteroid dehydrogenases; and 3- β HSD: 3 β -Hydroxysteroid dehydrogenases

3.4. Effects on Serum Lipid Profile

Rats exposed to As displayed a dyslipidemic profile characterized by a notable (P < 0.05) elevation in serum total cholesterol, triglycerides, and LDL-C, accompanied by a significant (P < 0.05) reduction in HDL-C compared to

controls (Figure 4A–D). Co-treatment with DIO substantially reversed this dyslipidemia, noticeably improving all lipid parameters compared to the As-only group. The lipid profile of the DIO-alone group remained normal and was not significantly different from that of the control group.

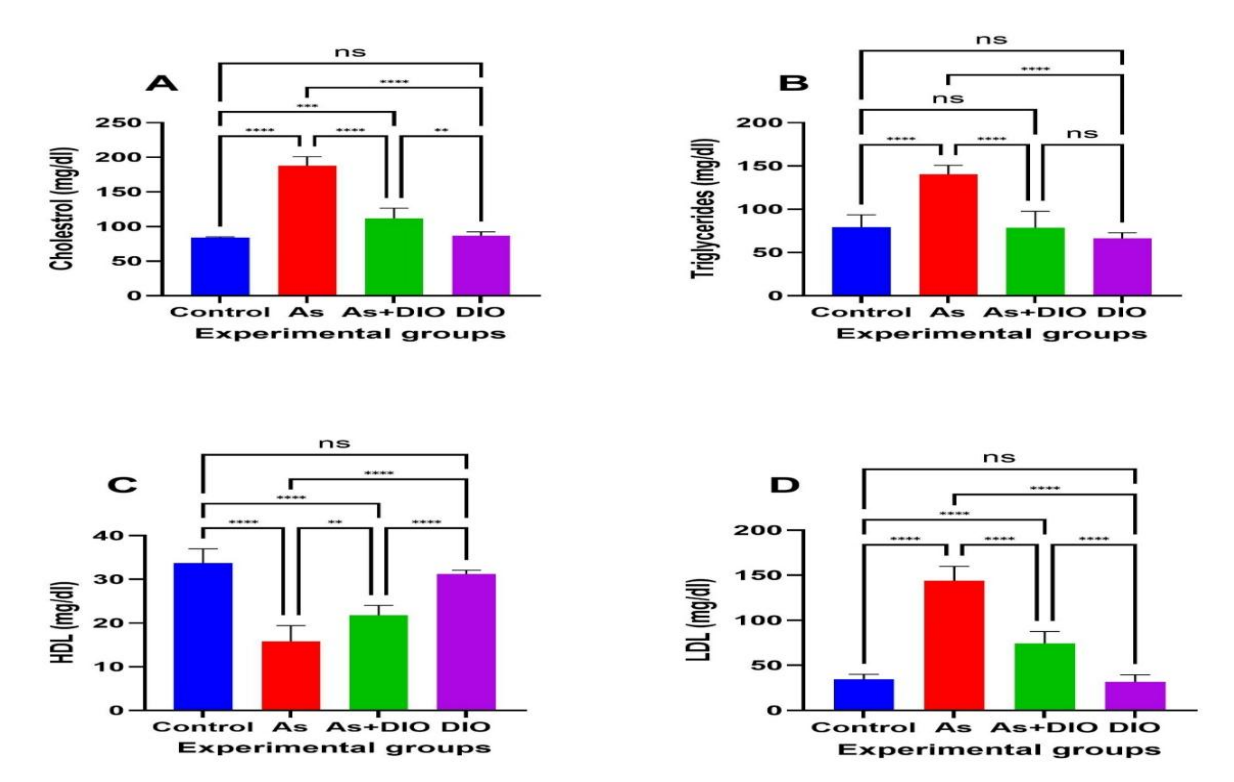
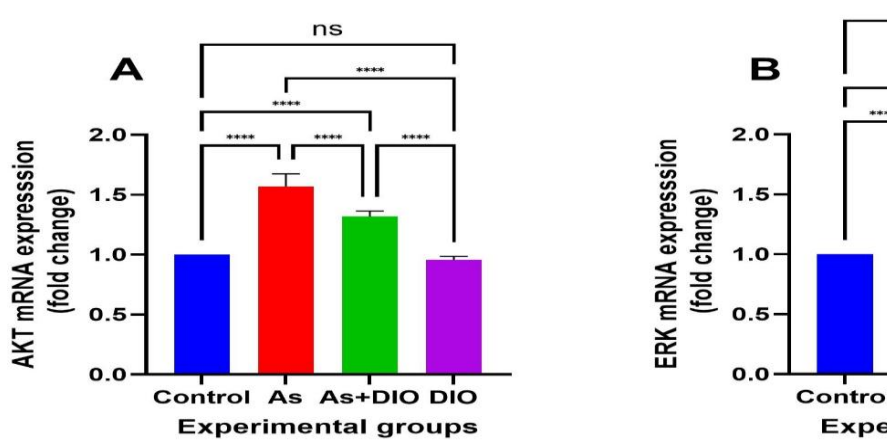


Figure (4) Assessment of Changes in the serum lipid profiles of experimental groups (**A**) Cholestrol, (**B**) Triglycerides, (C) HDL-C, and (**D**) LDL-C of animal groups. The results are exhibited as mean \pm SD when n =6, which were analyzed following one-way ANOVA associated with multiple comparisons between different groups adopting Tukey's test (**** p < 0.001, *** p < 0.001, *** p < 0.01, and * p < 0.05). Abbreviations: HDL-C: high-density lipoprotein cholesterol; and LDL-C: low-density lipoprotein cholesterol

3.5. Effects on Testicular Gene Expression

The gene expression levels of both Akt and ERK were considerably upregulated in the testicular tissue of the Astreated group relative to controls (Figure 5A, B). Cotreatment with DIO restrained this As-induced upregulation,

resulting in expression levels remarkably lower than those in the As-only group. The expression levels in the DIO-alone group showed no significant (P > 0.05) difference compared to controls.



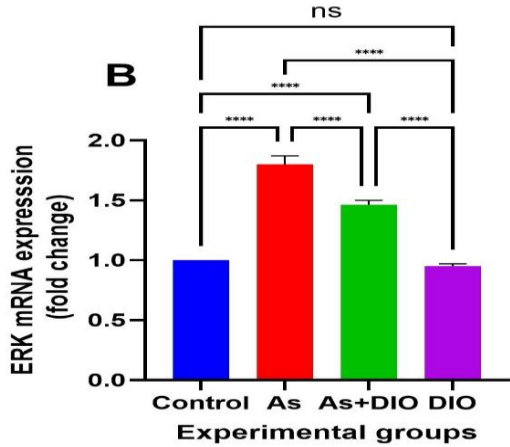


Figure (5) Determination of (**A, B**) mRNA expression of AKT and ERK in testicular tissues of different rat groups. The results are exhibited as mean \pm SD when n =5, which were analyzed following one-way ANOVA associated with multiple comparisons between different groups adopting Tukey's test (**** p < 0.0001, *** p < 0.001, *** p < 0.01, and * p < 0.05). Abbreviations Akt: protein kinase B; and ERK: extracellular signal-Regulated Kinase

3.6. Histopathological Observations

Histological findings demonstrated that As severely compromised the integrity of testicular tissues. Testes from control and DIO-alone rats displayed normal architecture, characterized by intact seminiferous tubules, well-organized spermatogenic cells, abundant spermatozoa within the lumen, and healthy interstitial Leydig cells (Figure 6A, D). In sharp contrast, testes from the As-treated group exhibited severe

damage, including vacuolization, cellular debris, and pyknotic nuclei. The seminiferous tubules were atrophied and had irregular outlines, while germ and Leydig cells were disorganized and degenerated (Figure 6B). Crucially, cotreatment with DIO effectively countered this damage, resulting in a noticeable restoration of testicular morphology, with restored tubule structure and a normal arrangement of spermatogenic and Leydig cells (Figure 6C).

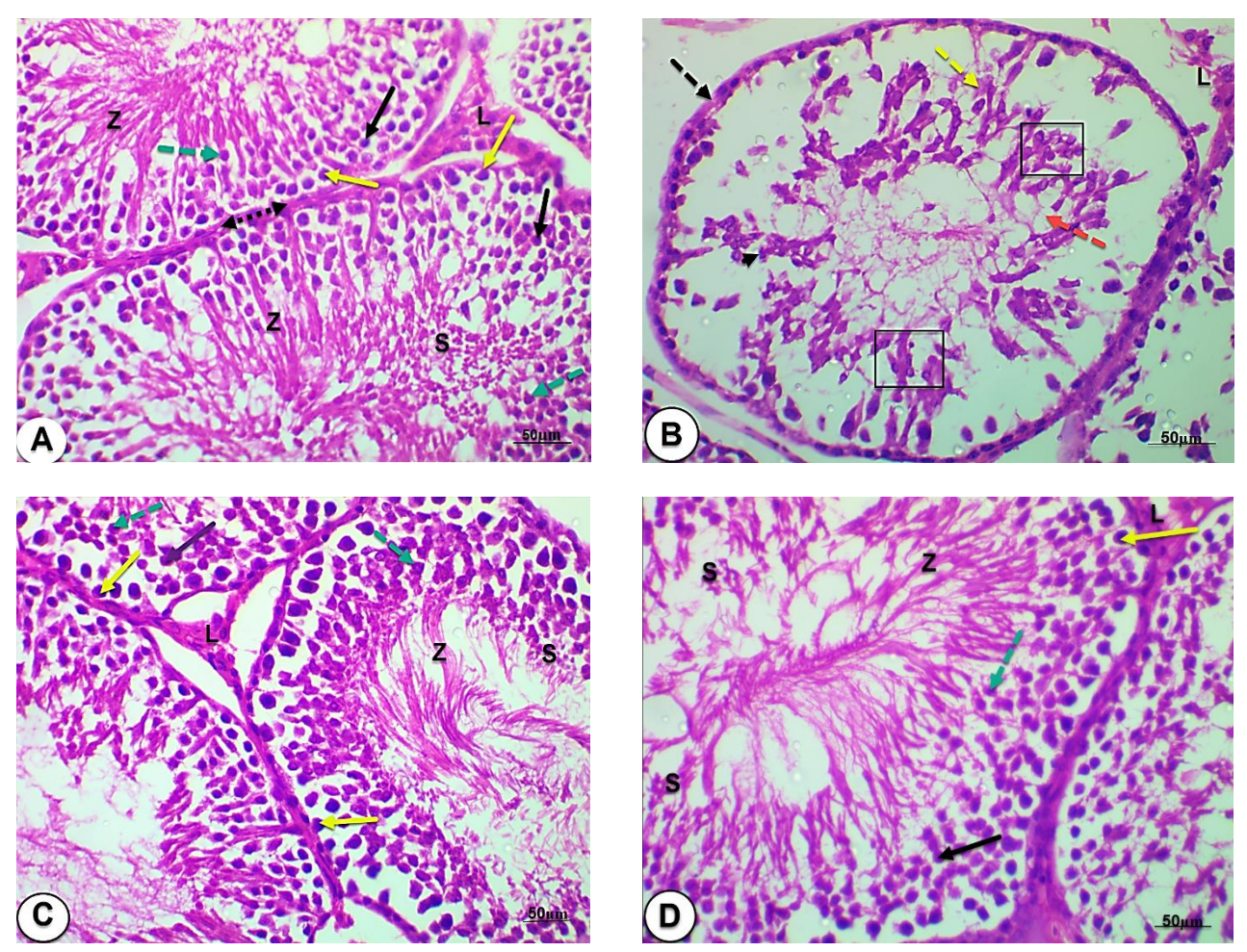


Figure 6: Representative photomicrographs of testicular tissue across experimental (A & D) Sections from control and DIO-alone rats reveal intact testicular structure, characterized by seminiferous tubules with normal morphology (black double-headed dotted arrow), healthy interstitial tissue with typical Leydig cells (L), and wellorganized spermatogenic series including spermatogonia (yellow arrow), primary spermatocytes (black arrow), secondary spermatocytes (green dotted arrow), spermatids (S), and spermatozoa occupying the luminal space (Z). (B) As-exposed group exhibits severe histopathological disruptions, including vacuolation (red dotted arrow), cellular debris deposition (yellow dotted arrow), nuclear pyknosis (black arrowhead), irregularly contoured atrophic tubules (black dotted arrow), degenerated/disarrayed germinal epithelium (black (C) Combined As + DIO treatment reveals substantial recovery, with seminiferous tubules regaining normal appearance, wellstructured spermatogenic layers, and preserved Leydig cells (L). (H&E ×400)

3.7. Immunohistochemical Analysis of Caspase-3

Immunohistochemical analysis for caspase-3 revealed stark differences between the groups. Testicular tissue from control and DIO-alone rats showed only weak caspase-3 immunoreactivity, indicating minimal cell death (Figure 7A,

D). In contrast, the As-treated group exhibited strong positive expression of caspase-3, confirming a high rate of apoptosis (Figure 7B). Notably, co-treatment with DIO significantly mitigated this effect, with caspase-3 immunoreactivity returning to levels similar to the control group (Figure 7C).

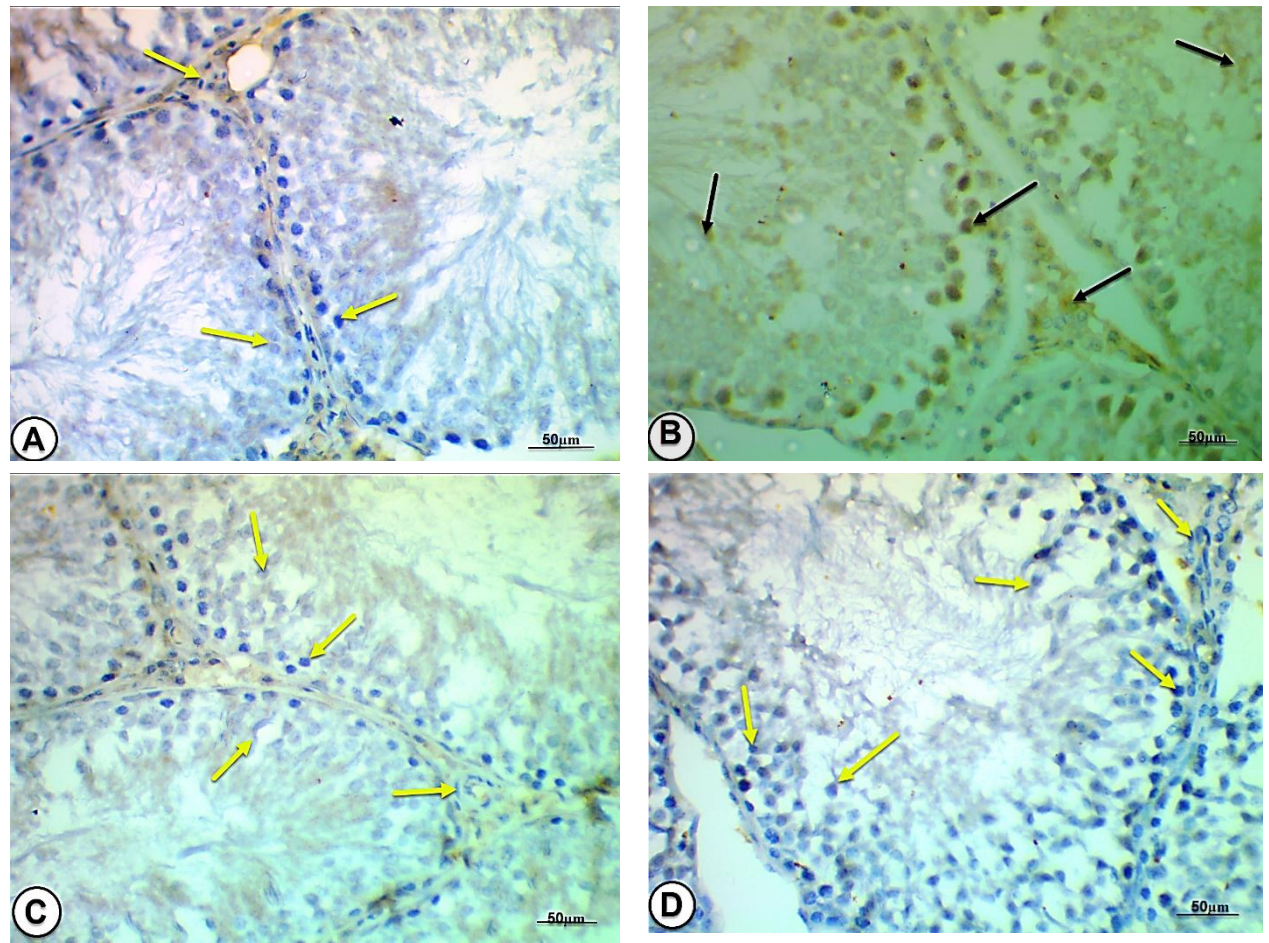


Figure 7: Representative Immuno histochemistry of caspase-3 in testes (\times 400). Control (A) and DIO (D) sections reveal faint expression. In the As group (B), robust caspase-3 reactivity is detected, indicating enhanced apoptosis. Co-treatment with DIO (C) reduces this response, with only few positive cells. Yellow arrows = negative; black arrows = positive.

4. Discussion

This investigation provides compelling evidence that sodium arsenite (As) exposure precipitates extensive reproductive dysfunction in male rats through a multi-faceted pathogenesis involving oxidative damage, inflammatory activation, endocrine disruption, metabolic dysregulation, and apoptotic cell death (Ganie et al., 2024; Choudhary et al., 2024). The experimental data further establish diosmin (DIO) as a potent therapeutic agent capable of counteracting these pathological alterations through its diverse pharmacologic activities (Malayeri et al., 2024).

The foundation of As-induced testicular injury appears to be rooted in profound oxidative stress, as demonstrated by the significant increase in TBARS and concomitant depletion of crucial antioxidant defenses (GSH, SOD, CAT). These findings align with those of Rachamalla et al. (2022) and Makena et al. (2025). This redox imbalance originates from arsenic's capacity to bind sulfhydryl groups in antioxidant enzymes and disrupt mitochondrial electron transport, culminating in excessive generation of reactive oxygen species (ROS) that damage cellular macromolecules and structures (Khan et al., 2013; Machado-Neves, 2022; Zargari et al., 2022; Eslami et al., 2024). Critically, co-administration of DIO with As effectively mitigated this oxidative assault,

not only reducing TBARS levels but also restoring antioxidant reserves. This dual action suggests DIO's polyphenolic structure confers direct free radical scavenging capabilities while potentially upregulating endogenous defense mechanisms, thereby preserving cellular integrity against As-induced peroxidative damage (Parhiz et al., 2015; Alkhalaf, 2020).

Testicular tissues of As-exposed rats exhibited marked inflammatory activation, as shown by increased NF- κ B and TNF- α levels. The observed activation of NF- κ B and TNF- α following As exposure reflects a robust inflammatory response (Escudero-Lourdes, 2016; Akbari et al., 2022), which is often secondary to oxidative stress. ROS activate NF- κ B, which in turn promotes the transcription of proinflammatory cytokines like TNF- α , creating a vicious cycle of oxidative—inflammatory damage.

Conversely, DIO co-treatment effectively mitigated this inflammatory cascade, maintaining NF- κ B and TNF- α levels significantly below those observed in the As-only group. DIO's anti-inflammatory potential seems to stem largely from its antioxidant capacity. Research indicates that flavonoids can inhibit NF- κ B signaling (Elhelaly et al., 2019), and for DIO, this effect is likely mediated by its ability to reduce oxidative stress (Parhiz et al., 2015; Mohtadi

et al., 2023). By lowering ROS levels, DIO removes the primary trigger that initiates the pro-inflammatory response, thereby dampening the cascade of inflammation.

Moreover, As exposure markedly compromised male reproductive function, as reflected by reduced sperm count and motility and increased abnormal sperm morphology. These functional impairments were accompanied by a significant decline in serum GnRH, FSH, LH, and testosterone levels, as well as suppressed activities of steroidogenic enzymes 17β-HSD and 3β-HSD. The impairment of sperm quality and the reduction in key reproductive hormones and steroidogenic enzymes in Astreated rats illustrate the functional consequences of this cellular damage (Khan et al., 2013; Machado-Neves, 2022; Makena et al., 2025). As markedly lowers sperm count and motility while increasing the proportion of morphologically abnormal sperm. These defects, often associated with oxidative stress and DNA damage in developing germ cells, hinder fertilization potential (Machado-Neves, 2022). As also disrupts the hypothalamic-pituitary-gonadal (HPG) axis, leading to reduced secretion of GnRH, decreased FSH and LH, and lowered testosterone production by Leydig cells (Zargari et al., 2022). The decline in testosterone results not only from direct Leydig cell damage but also from inhibited activity of 3β-HSD and 17β-HSD, which are essential for testosterone biosynthesis (Zargari et al., 2022; Makena et al., 2025).

Conversely, As + DIO rats showed notable improvement in all reproductive deficits. By mitigating oxidative stress, DIO protects germ cells and supports steroidogenic function (Abou-Elghait et al., 2022). Its effect may also involve the modulation of signaling pathways that upregulate steroidogenic enzyme expression, as seen with other flavonoids (Ni et al., 2020; Khamis et al., 2023; Deiab et al., 2024).

The present data indicate that As-induced dyslipidemia (elevated cholesterol, triglycerides, LDL-C; reduced HDL-C) (Pánico et al., 2022) further exacerbates reproductive toxicity. Lipid peroxidation products and dysregulated cholesterol metabolism can impair Leydig cell function (Jing et al., 2020). In contrast, DIO co-treatment successfully reversed these detrimental effects. DIO's ability to improve the lipid profile is multifaceted, involving antioxidant protection of the liver, anti-inflammatory actions that prevent cytokine-driven dyslipidemia, and potential activation of nuclear receptors like PPAR- α to promote lipid catabolism and reverse cholesterol transport (Parhiz et al., 2015; Elhelaly et al., 2019; Chung et al., 2020; Ding et al., 2024).

The observed upregulation of Akt and ERK gene expression after As exposure appears to be a maladaptive response to oxidative stress (Huang et al., 2016; Renu et al., 2018). While these pathways are essential for cell survival, their sustained activation can paradoxically drive apoptosis and disrupt spermatogenesis (Mukherjee & Gopalakrishnan, 2023). By contrast, the elevated expression caused by As exposure was counteracted by DIO co-treatment, which markedly reduced the levels compared to the As-only group. DIO's ability to normalize the expression of these genes suggests it modulates

critical survival signaling pathways, likely by alleviating the initial oxidative insult and potentially through direct inhibitory effects on the PI3K/Akt axis, as reported for similar compounds (Do Amaral et al., 2011; Rubio et al., 2012; Sarhan et al., 2021; Deng et al., 2022).

Exposure to As resulted in profound histopathological lesions within the testes, manifested by marked vacuolization, accumulation of cellular debris, condensed and pyknotic nuclei, shrunken seminiferous tubules with distorted contours, and extensive degeneration of both germinal and Leydig cell populations. These alterations were corroborated intense caspase-3 immunoreactivity, pronounced apoptotic activity. The severe histopathological damage and intense caspase-3 immunoreactivity in the As group provide morphological and biochemical proof of widespread apoptosis and testicular failure (Zargari et al., 2022; Li et al., 2018; Adeogun et al., 2025). Conversely, rats co-administered with DIO retained largely preserved testicular cytoarchitecture, with reduced vacuolization and cellular degeneration, alongside a noticeably weaker caspase-3 expression. The restoration of testicular architecture and suppression of caspase-3 activation in the DIO group offer compelling evidence of its therapeutic potential (Oyovwi et al., 2024). DIO's anti-apoptotic effect is achieved by restoring the redox balance, inhibiting mitochondrial cytochrome c release, modulating Bcl-2 family proteins, and suppressing pro-apoptotic signaling pathways (Shalkami et al., 2018; Ağır & Eraslan, 2019; Koolaji et al., 2020; Hong & An, 2018).

4. Conclusion

This research provides compelling evidence that DIO serves as a potent protective agent against the multifaceted reproductive impairments induced by As in male rats. The observed benefits including restored sperm parameters, normalized GnRH-FSH-LH-testosterone axis function, and preserved steroidogenic enzyme activity are strongly linked to DIO's ability to reduce oxidative stress and attenuate inflammatory responses within testicular Furthermore, the successful modulation of disrupted Akt/ERK signaling by DIO points to its influence on crucial cellular survival and proliferation pathways. Collectively, these findings illuminate the complex interplay between arsenic toxicity and cellular defense mechanisms, positioning DIO as a promising natural therapeutic candidate. Future investigations should focus on translating these preclinical insights into clinical applications, exploring optimal dosing regimens, and elucidating additional molecular targets to further enhance strategies for male reproductive health protection in arsenic-contaminated regions.

Acknowledgements

Not applicable.

Conflicts of interest

The authors declare no competing interests.

Funding

No funding sources.

References

Abou-Elghait, A. T., Elgamal, D. A., Abd el-Rady, N. M., Hosny, A., & Ali, F. E. (2022). Novel protective effect of diosmin against cisplatin-induced prostate and seminal vesicle damage: role of oxidative stress and apoptosis. Tissue and Cell, 79, 101961.

- Adeogun, A. E., Ogunleye, O. D., Akhigbe, T. M., Oyedokun, P. A., Adegbola, C. A., Saka, W. A., ... & Akhigbe, R. E. (2025). Impact of arsenic on male and female reproductive function: A review of the pathophysiology and potential therapeutic strategies. Naunyn-Schmiedeberg's Archives of Pharmacology, 398(2), 1283-1297. https://doi.org/10.1007/s00210-024-03323-0
- Aebi, H. (1984). Catalase in vitro. Methods in Enzymology, 105, 121–126. https://doi.org/10.1016/S0076-6879 (84)05016-3
- Ağır, M. S., & Eraslan, G. (2019). The effect of diosmin against liver damage caused by cadmium in rats. Journal of Food Biochemistry, 43 (9), e12966. https://doi.org/10.1111/jfbc.12966
- Ahmed, S., Mundhe, N., Borgohain, M., Chowdhury, L., Kwatra, M., Bolshette, N., ... & Lahkar, M. (2016). Diosmin modulates the NF-kB signal transduction pathways and downregulation of various oxidative stress markers in alloxan-induced diabetic nephropathy. Inflammation, 39 (5), 1783–1797. https://doi.org/10.1007/s10753-016-0416-1
- Akbari, S., Amiri, F. T., Naderi, M., Shaki, F., & Seyedabadi, M. (2022). Sodium arsenite accelerates D-galactose-induced aging in the testis of the rat: Evidence for mitochondrial oxidative damage, NF-kB, JNK, and apoptosis pathways. Toxicology, 470, 153148. https://doi.org/10.1016/j.tox.2022.153148
- Alkhalaf, M. I. (2020). Diosmin protects against acrylamide-induced toxicity in rats: Roles of oxidative stress and inflammation. Journal of King Saud University-Science, 32 (2), 1510–1515. https://doi.org/10.1016/j.jksus.2019.12.007
- Allain, C. C., Poon, L. S., Chan, C. S., Richmond, W. F. P. C., & Fu, P. C. (1974). Enzymatic determination of total serum cholesterol. Clinical Chemistry, 20 (4), 470–475.
- Anwar, H. M., Hamad, S. R., Salem, G. E. M., Soliman, R. H. M., & Elbaz, E. M. (2022). Inflammatory modulation of miR-155 inhibits doxorubicin-induced testicular dysfunction via SIRT1/FOXO1 pathway: Insight into the role of acacetin and Bacillus cereus protease. Applied Biochemistry and Biotechnology, 194 (11), 5196–5219. https://doi.org/10.1007/s12010-022-03998-2
- Anwar, N., & Qureshi, I. Z. (2019). In vitro application of sodium arsenite to mice testicular and epididymal organ cultures induces oxidative, biochemical, hormonal, and genotoxic stress. Toxicology and Industrial Health, 35 (10), 660–669. https://doi.org/10.1177/07482337198743

Balkwill, F. (2009). Tumour necrosis factor and cancer. Nature Reviews Cancer, 9 (5), 361–371. https://doi.org/10.1038/nrc2628

- Beutler, E., Duron, O., & Kelly, B. M. (1963). Improved method for determination of blood glutathione. Journal of Laboratory and Clinical Medicine, 61, 882–888.
- Choudhary, A., Pandey, R., Rathod, D., Sumalatha, S., Murti, K., Ravichandiran, V., & Kumar, N. (2024). Dehydrozingerone ameliorates arsenic-induced reproductive toxicity in male Wistar rats. Journal of Molecular Histology, 55 (6), 1131–1145. https://doi.org/10.1007/s10735-024-10223-3
- Chung, S., Kim, H. J., Choi, H. K., Park, J. H., & Hwang, J. T. (2020). Comparative study of the effects of diosmin and diosmetin on fat accumulation, dyslipidemia, and glucose intolerance in mice fed a high-fat high-sucrose diet. Food Science & Nutrition, 8 (11), 5976–5984. https://doi.org/10.1002/fsn3.1893
- Deiab, N. S., Kodous, A. S., Mahfouz, M. K., Said, A. M., Ghobashy, M. M., & Abozaid, O. A. (2024). Smart hesperidin/chitosan nanogel mitigates apoptosis and endoplasmic reticulum stress in fluoride and aluminum-induced testicular injury. Biological Trace Element Research, 202 (9), 4106–4124. https://doi.org/10.1007/s12011-023-04033-1
- Deng, J., Zheng, C., Hua, Z., Ci, H., Wang, G., & Chen, L. (2022). Diosmin mitigates high glucose-induced endoplasmic reticulum stress through PI3K/AKT pathway in HK-2 cells. BMC Complementary Medicine and Therapies, 22(1), 116. https://doi.org/10.1186/s12906-022-03595
- Ding, J., Chen, F. P., Song, Y. Y., Li, H. Y., Ai, X. W., Chen, Y., ... & Guan, Y. T. (2024). Serum low-density lipoprotein cholesterol levels are associated with relapse in neuromyelitis optica spectrum disorder. Journal of Inflammation Research, 17, 8227–8240. https://doi.org/10.2147/JIR.S481073
- Do Amaral, C. L., Burim, R. V., Queiroz, R. H. C., Bianchi, M. D. L. P., & Antunes, L. M. G. (2011).
 The effects of dietary supplementation of methionine on genomic stability and p53 gene promoter methylation in rats. Mutation Research/Genetic Toxicology and Environmental Mutagenesis, 722 (1), 78–83
 - https://doi.org/10.1016/j.mrgentox.2011.03.005
- Draper, H. H., & Hadley, M. (1990). Malondialdehyde determination as index of lipid Peroxidation. Methods in Enzymology, 186, 421–431. https://doi.org/10.1016/0076-6879 (90)86135-I
- Elhelaly, A. E., AlBasher, G., Alfarraj, S., Almeer, R., Bahbah, E. I., Fouda, M. M., ... & Abdel-Daim, M. M. (2019). Protective effects of hesperidin and diosmin against acrylamide-induced liver, kidney, and brain oxidative damage in rats. Environmental Science and Pollution Research, 26 (34), 35151–35162. https://doi.org/10.1007/s11356-019-06622-9
- Escudero-Lourdes, C. (2016). Toxicity mechanisms of arsenic that are shared with neurodegenerative

- diseases and cognitive impairment: Role of oxidative stress and inflammatory responses. Neurotoxicology, 53, 223–235. https://doi.org/10.1016/j.neuro.2016. 02.002
- Eslami, H., Askari, F. R., Mahdavi, M., Taghavi, M., & Ghaseminasab-Parizi, M. (2024). Environmental arsenic exposure and reproductive system toxicity in male and female and mitigatory strategies: A review. Environmental Geochemistry and Health, 46 (10), 420. https://doi.org/10.1007/s10653-024-02152-9
- Essawy, A., Matar, S., Mohamed, N., Abdel-Wahab, W., & Abdou, H. (2024). Ginkgo biloba extract protects against tartrazine-induced testicular toxicity in rats: Involvement of antioxidant, anti-inflammatory, and anti-apoptotic mechanisms. Environmental Science and Pollution Research, 31 (10), 15065–15077. https://doi.org/10.1007/s11356-024-32263-8
- Fossati, P., & Prencipe, L. (1982). Serum triglycerides determined colorimetrically with an enzyme that produces hydrogen peroxide. Clinical Chemistry, 28 (10), 2077–2080.
- Friedewald, W. T., Levy, R. I., & Fredrickson, D. S. (1972). Estimation of the concentration of low-density lipoprotein cholesterol in plasma, without use of the preparative ultracentrifuge. Clinical Chemistry, 18 (6), 499–502.
- Ganie, S. Y., Javaid, D., Hajam, Y. A., & Reshi, M. S. (2024). Arsenic toxicity: Sources, pathophysiology and mechanism. Toxicology Research, 13(1), tfad111. https://doi.org/10.1093/toxres/tfad111
- Guo, J., Chen, S., Zhang, Y., Liu, J., Jiang, L., Hu, L., ... & Chen, X. (2024). Cholesterol metabolism: Physiological regulation and diseases. MedComm, 5 (2), e476, https://doi.org/10.1002/mco2.476
- Habib, C. N., Mohamed, M. R., Tadros, M. G., Tolba, M. F., Menze, E. T., & Masoud, S. I. (2022). The potential neuroprotective effect of diosmin in rotenone-induced model of Parkinson's disease in rats. European Journal of Pharmacology, 914, 174573. https://doi.org/10.1016/j.ejphar.2021.174573
- Han, G., Xuanyuan, S., Zhang, B., & Shi, C. (2022). Activation of PI3K/Akt prevents hypoxia/reoxygenation-induced GnRH decline via FOXO3a. Physiological Research, 71 (4), 509–519. https://doi.org/10.33549/physiolres.934873
- Hassan, M. A., Elmageed, G. M. A., El-Qazaz, I. G., El-Sayed, D. S., El-Samad, L. M., & Abdou, H. M. (2023). The synergistic influence of polyflavonoids from Citrus aurantifolia on diabetes treatment and their modulation of the PI3K/AKT/FOXO1 signaling pathways: Molecular docking analyses and in vivo investigations. Pharmaceutics, 15 (9), 2306. https://doi.org/10.3390/pharmaceutics15092306
- Hong, Y., & An, Z. (2018). Hesperidin attenuates learning and memory deficits in APP/PS1 mice through activation of Akt/Nrf2 signaling and inhibition of RAGE/NF-κB signaling. Archives of Pharmacal

- Research, 41 (6), 655–663. https://doi.org/10.1007/s12272-018-1032-4
- Hsu, S. M., Raine, L., & Fanger, H. (1981). Use of avidinbiotin-peroxidase complex (ABC) immunoperoxidase techniques: comparison between ABC and unlabeled antibody (PAP) Journal procedures. Histochemistry of 29 Cytochemistry, (4),577-580. https://doi.org/10.1177/29.4.6166661
- Huang, Q., Luo, L., Alamdar, A., Zhang, J., Liu, L., Tian, M., ... & Shen, H. (2016). Integrated proteomics and metabolomics analysis of rat testis: Mechanism of arsenic-induced male reproductive toxicity. Scientific Reports, 6 (1), 32518. https://doi.org/10.1038/srep32518
- Hwang, Y. Y., Sudirman, S., Wei, E. Y., Shiu, R. F., Kong,
 Z. L., & Hwang, D. F. (2025). Yamabushitake
 Mushroom (Hericium erinaceus (Bull.) Pers. 1797)
 Mycelium Improves Reproductive System
 Dysfunction in Male Rats Induced by Polystyrene
 Microplastics. International Journal of Molecular
 Sciences, 26 (12), 5735. https://doi.org/10.3390/ijms
 26125735
- Jing, J., Ding, N., Wang, D., Ge, X., Ma, J., Ma, R., ... & Yao, B. (2020). Oxidized-LDL inhibits testosterone biosynthesis by affecting mitochondrial function and the p38 MAPK/COX-2 signaling pathway in Leydig cells. Cell Death & Disease, 11 (8), 626. https://doi.org/10.1038/s41419-020-02866-3
- Khamis, T., Hegazy, A. A., El-Fatah, S. S. A., Abdelfattah, E. R., Abdelfattah, M. M. M., Fericean, L. M., & Arisha, A. H. (2023). Hesperidin mitigates cyclophosphamide-induced testicular dysfunction via altering the hypothalamic pituitary gonadal axis and testicular steroidogenesis, inflammation, and apoptosis in male rats. Pharmaceuticals, 16 (2), 301. https://doi.org/10.3390/ph16020301
- Khan, S., Telang, A. G., & Malik, J. K. (2013). Arsenic-induced oxidative stress, apoptosis and alterations in testicular steroidogenesis and spermatogenesis in wistar rats: Ameliorative effect of curcumin. World Journal of Pharmacy and Pharmaceutical Sciences, 2 (3), 33-48.
- Koolaji, N., Shammugasamy, B., Schindeler, A., Dong, Q., Dehghani, F., & Valtchev, P. (2020). Citrus peel flavonoids as potential cancer prevention agents. Current Developments in Nutrition, 4 (5), nzaa025. https://doi.org/10.1093/cdn/nzaa025
- Kozłowska, A., Wojtacha, P., Równiak, M., Kolenkiewicz, M., & Huang, A. C. W. (2019). ADHD pathogenesis in the immune, endocrine and nervous systems of juvenile and maturating SHR and WKY rats. Psychopharmacology, 236 (10), 2937–2958. https://doi.org/10.1007/s00213-019-5176-9
- Lawrence, T. (2009). The nuclear factor NF-κB pathway in inflammation. Cold Spring Harbor Perspectives in Biology, 1 (6), a001651. https://doi.org/10.1101/cshperspect.a001651

Li, D., Wei, Y., Xu, S., Niu, Q., Zhang, M., Li, S., & Jing, M. (2018). A systematic review and meta-analysis of bidirectional effect of arsenic on ERK signaling pathway. Molecular Medicine Reports, 17 (3), 4422–4432. https://doi.org/10.3892/mmr.2018.8448

- Livak, K. J., & Schmittgen, T. D. (2001). Analysis of relative gene expression data using real-time quantitative PCR and the $2-\Delta\Delta CT$ method. Methods, 25 (4), 402–408. https://doi.org/10.1006/meth.2001.1262
- Lopes-Virella, M. F., Stone, P., Ellis, S., & Colwell, J. A. (1977). Cholesterol determination in high-density lipoproteins separated by three different methods. Clinical Chemistry, 23 (5), 882–884.
- Machado-Neves, M. (2022). Arsenic exposure and its implications in male fertility. Animal Reproduction, 19 (4), e20220119. https://doi.org/10.1590/1984-3143-ar2022-0119
- Mahmoud, S. A., El-Ghareeb, A. E. W., & Abd El-Rahman, H. A. (2025). Chlorantraniliprole (Coragen® 20% SC) exposure induced reproductive toxicity mediated by oxidative stress, apoptosis, and sperm quality deficient in male Wistar rats. Naunyn-Schmiedeberg's Archives of Pharmacology, 398 (2), 1283–1297. https://doi.org/10.1007/s00210-024-03323-0
- Makena, W., Anthony Bazabang, S., Tabakwot Ayuba, J., Nwankwo, M., Danchal Vandu, C., & Bakri Idris Attalla, N. (2025). Mechanistic insights into the protective role of Senna occidentalis extract in mitigating sodium arsenite-induced testicular toxicity. International Journal of Environmental Health Research, 1-14. https://doi.org/10.1080/09603123.2024.2429293
- Malayeri, A., Birgani, S. M., Basir, Z., & Kalantar, H. (2024). Protective effects of diosmin on doxorubicininduced testicular toxicity in rat. Naunyn-Schmiedeberg's Archives of Pharmacology, 397 (10), 7881–7890. https://doi.org/10.1007/s00210-024-03046-2
- Martin, L. J., & Touaibia, M. (2020). Improvement of testicular steroidogenesis using flavonoids and isoflavonoids for prevention of late-onset male hypogonadism. Antioxidants, 9 (3), 237. https://doi.org/10.3390/antiox9030237
- Mishra, R., Nikam, A., Hiwarkar, J., Nandgude, T., Bayas, J., & Polshettiwar, S. (2024). Flavonoids as potential therapeutics in male reproductive disorders. Future Journal of Pharmaceutical Sciences, 10 (1), 100. https://doi.org/10.1186/s43094-024-00668-4
- Mohtadi, S., Shariati, S., Mansouri, E., & Khodayar, M. J. (2023). Nephroprotective effect of diosmin against sodium arsenite-induced renal toxicity is mediated via attenuation of oxidative stress and inflammation in mice. Pesticide Biochemistry and Physiology, 197, 105652.
 - https://doi.org/10.1016/j.pestbp.2023.105652
- Morakinyo, A. O., Achema, P. U., & Adegoke, O. A. (2010). Effect of Zingiber officinale (Ginger) on

sodium arsenite-induced reproductive toxicity in male rats. African Journal of Biomedical Research, 13 (1), 39–45.

- Mukherjee, A. G., & Gopalakrishnan, A. V. (2023). The interplay of arsenic, silymarin, and NF-κB pathway in male reproductive toxicity: A review. Ecotoxicology and Environmental Safety, 252, 114614. https://doi.org/10.1016/j.ecoenv.2023.114614
- Ni, G., Zhang, X., Afedo, S. Y., & Rui, R. (2020). Evaluation of the protective effects of icariin on nicotine-induced reproductive toxicity in male mouse—a pilot study. Reproductive Biology and Endocrinology, 18 (1), 56. https://doi.org/10.1186/s12958-020-00617-9
- Nishikimi, M., Rao, N. A., & Yagi, K. (1972). The occurrence of superoxide anion in the reaction of reduced phenazine methosulfate and molecular oxygen. Biochemical and biophysical research communications, 46(2), 849-854.
- Oguzoglu, A. S., Asci, H., Tepebasi, M. Y., Ilhan, I., Canan, M., Senol, N., ... & Ozmen, O. (2024). The role of different antioxidant pathways like AKT, SIRT-1, NRF2 and HO-1 in cardiac damage after subarachnoid hemorrhage. Turkish Neurosurgery, 34 (6), 856-865. https://doi.org/10.5137/1019-5149.JTN.45300-23.2
- Olojede, S. O., Lawal, S. K., Faborode, O. S., Dare, A., Aladeyelu, O. S., Moodley, R., ... & Azu, O. O. (2022). Testicular ultrastructure and hormonal changes following administration of tenofovir disoproxil fumarate-loaded silver nanoparticle in type-2 diabetic rats. Scientific Reports, 12 (1), 9633. https://doi.org/10.1038/s41598-022-13675-3
- Oyovwi, M. O., Ben-Azu, B., Tesi, E. P., Ojetola, A. A., Olowe, T. G., Joseph, U. G., ... & Falajiki, F. Y. (2024). Diosmin protects the testicles from doxorubicin-induced damage by increasing steroidogenesis and suppressing oxido-inflammation and apoptotic mediators. International Journal of Biochemistry and Molecular Biology, 15 (2), 34–50.
- Pánico, P., Velasco, M., Salazar, A. M., Picones, A., Ortiz-Huidobro, R. I., Guerrero-Palomo, G., ... & Hiriart, M. (2022). Is arsenic exposure a risk factor for metabolic syndrome? A review of the potential mechanisms. Frontiers in Endocrinology, 13, 952465. https://doi.org/10.3389/fendo.2022.952465
- Parhiz, H., Roohbakhsh, A., Soltani, F., Rezaee, R., & Iranshahi, M. (2015). Antioxidant and anti-inflammatory properties of the citrus flavonoids hesperidin and hesperetin: An updated review of their molecular mechanisms and experimental models. Phytotherapy Research, 29 (3), 323–331. https://doi.org/10.1002/ptr.5256
- Rachamalla, M., Chinthada, J., Kushwaha, S., Putnala, S. K., Sahu, C., Jena, G., & Niyogi, S. (2022). Contemporary comprehensive review on arsenic-induced male reproductive toxicity and mechanisms

- of phytonutrient intervention. Toxics, 10 (12), 744. https://doi.org/10.3390/toxics10120744
- Ramalingam, M., Kwon, Y. D., & Kim, S. J. (2016). Insulin as a potent stimulator of Akt, ERK and Inhibin-βE signaling in osteoblast-like UMR-106 cells. Biomolecules & Therapeutics, 24 (6), 589–594. https://doi.org/10.4062/biomolther.2016.120
- Renu, K., Madhyastha, H., Madhyastha, R., Maruyama, M., Vinayagam, S., & Gopalakrishnan, A. V. (2018). Review on molecular and biochemical insights of arsenic-mediated male reproductive toxicity. Life Sciences, 212, 37–58. https://doi.org/10.1016/j.lfs.2018.09.045
- Rubio, S., León, F., Quintana, J., Cutler, S., & Estévez, F. (2012). Cell death triggered by synthetic flavonoids in human leukemia cells is amplified by the inhibition of extracellular signal-regulated kinase signaling. European Journal of Medicinal Chemistry, 55, 284–296. https://doi.org/10.1016/j.ejmech.2012. 07.030
- Sarhan, H. K., Saleh, A. M., Hammam, O., Atta, A. H., & Elnahrery, E. (2021). The protective role of Diosmin, Hesperidine combination against heavy metals toxicity in Wistar albino rats: Biochemical, Immunohistochemical and Molecular Studies. Egyptian Journal of Chemistry, 64 (8), 4531–4543. https://doi.org/10.21608/ejchem.2021.69430.3558

- Shalkami, A. S., Hassan, M. I. A., & Bakr, A. G. (2018). Anti-inflammatory, antioxidant and anti-apoptotic activity of diosmin in acetic acid-induced ulcerative colitis. Human & Experimental Toxicology, 37 (1), 78–86. https://doi.org/10.1177/0960327116689714
- Slott, V. L., Suarez, J. D., & Perreault, S. D. (1991). Rat sperm motility analysis: Methodologic considerations. Reproductive Toxicology, 5 (5), 449–458. https://doi.org/10.1016/0890-6238 (91)90005-8
- Tappel, A. L., & Zalkin, H. (1959). Lipide peroxidation in isolated mitochondria. Archives of Biochemistry and Biophysics, 80 (2), 326–332. https://doi.org/10.1016/0003-9861(59)90214-4
- Wang, J., Zhu, H., Lin, S., Wang, K., Wang, H., & Liu, Z. (2021). Protective effect of naringenin against cadmium-induced testicular toxicity in male SD rats. Journal of Inorganic Biochemistry, 214, 111310. https://doi.org/10.1016/j.jinorgbio.2020.111310
- Yao, Y., Chang, X., Wang, D., Ma, H., Wang, H., Zhang, H., ... & Wang, J. (2018). Roles of ERK1/2 and PI3K/AKT signaling pathways in mitochondriamediated apoptosis in testes of hypothyroid rats. Toxicology Research, 7 (6), 1214–1224. https://doi.org/10.1039/C8TX00130F
- Zargari, F., Rahaman, M. S., KazemPour, R., & Hajirostamlou, M. (2022). Arsenic, oxidative stress and reproductive system. Journal of Xenobiotics, 12 (3), 214–222. https://doi.org/10.3390/jox12030018.